JOURNAL OF Materials CHEMISTRY Feature Article

Lithium ion mobility in metal oxides: a materials chemistry perspective†

Litty Sebastian and J. Gopalakrishnan*

Solid State and Structural Chemistry Unit, Indian Institute of Science, Bangalore 560 012, India. E-mail: gopal@sscu.iisc.ernet.in

Received 19th November 2002, Accepted 10th January 2003
First published as an Advance Article on the web 22nd January 2003

Metal oxides containing mobile lithium ions are technologically important materials in the context of design and development of electrolytes and electrodes for solid-state lithium batteries. Mobility of lithium in a solid manifests itself in the following measureable ways: ionic conductivity/diffusion, redox insertion/deinsertion and ion exchange. While ionic conductivity and redox insertion/deinsertion determine the practical use of a material as an electrolyte and electrodes, respectively, ion exchange involving lithium in aqueous/molten salt media under mild conditions not only provides a convenient probe for the investigation of lithium mobility in solids, but also enables synthesis of new metastable phases. In this article, we present a chemical (rather than electrochemical) perspective of lithium ion mobility in inorganic oxide materials, in an attempt to bring out the relationships between structure and properties associated with lithium ion mobility. The survey shows that considerable lithium ion mobility occurs both in close-packed (rocksalt and its relatives, spinel, $LiNbO_3$, rutile and perovskite) as well as open-framework (*e.g.* NASICON) oxide structures. $LiCoO_2$ (α-$NaFeO_2$), $LiMn_2O_4$ (spinel), $LiNbO_3$/$LiTaO_3$ (structure based on HCP array of anions), $LiNbWO_6$ (trirutile) and (Li,La)TiO_3 (perovskite) are some of the oxide materials (structure type indicated in parentheses) where high lithium mobility has been well established by various experimental studies. An investigation of the factors that control lithium ion conductivity in the (Li,La)TiO_3 perovskite has enabled us to design new perovskite oxides in the Li–Sr–B–B′–O (B = Ti, Zr; B′ = Nb, Ta) systems that exhibit high lithium ion mobility/conductivity. Among the framework materials, NASICON (*e.g.* $Na_3Zr_2PSi_2O_{12}$) turns out to be a versatile structure that supports high lithium mobility under ion-exchange, ionic conductivity and redox insertion/deinsertion conditions.

1 Introduction

Inorganic solids containing mobile lithium ions are important materials for the development of lithium batteries.[1] Solids where lithium ion mobility is accompanied by a redox process are useful as *electrodes*, whereas solids where a concerted ion migration occurs under the influence of an electric field (that gives rise to ionic conductivity) are useful as *electrolytes* for lithium batteries.[1] Research and development[2,3] over the past 30 years have identified two definite oxide materials, $LiCoO_2$ and $LiMn_2O_4$, which are already in use as cathodes in commercial rechargeable lithium batteries. As for the anode, graphite remains the best material for lithium ion (rocking chair) batteries.[2,3]

As for the electrolyte, we do have a large number of inorganic solids exhibiting high lithium ion conductivity,[4,5] but commercial lithium batteries at present make use of organic liquid/polymer-based electrolytes,[1,6] for technological reasons. Current research effort is directed toward finding better materials in terms of cost, energy density and safety for all the three constituents of a lithium battery.[1,6] In the search for lithium battery materials, metal oxides exhibiting high lithium mobility offer attractive opportunities.

High lithium mobility manifests itself in several measureable ways,[7] including diffusion, ionic conductivity and ion exchange. While the relationship between diffusion and ionic conductivity in inorganic solids is well established through the Nernst–Einstein relation (conductivity, $\sigma = Ne^2D/kT$, where D is the diffusion coefficient of the conducting ion and N its number per unit volume), the relationship between ionic conductivity and ion exchange is not as straightforward. England *et al.*,[8] who investigated the problem of ion exchange in inorganic oxides, point out the details: while ionic conduction involves single ion diffusion coefficients, ion exchange depends on interdiffusion coefficients, involving both the in-coming and out-going ions. Also, the crystal structure plays a crucial role in defining migration pathways. The kinetic (activation) barriers for both processes may not be the same. Therefore, a fast ion-conducting solid does not necessarily undergo fast ion exchange.[9] For example, NASICON ($Na_3Zr_2PSi_2O_{12}$) which is a well-known fast sodium ion conductor, does not undergo facile ion exchange; it requires forcing conditions for ion exchange with other monovalent cations. Similarly, a facile ion-exchange material is not necessarily a fast ion conductor. A case in point is $LiTi_2(PO_4)_3$, where Li^+/H^+ exchange is facile, but conductivity is poor.

The work of England *et al.*[8] has shown that ion exchange is quite a widespread phenomenon among several inorganic solids, considerable exchange occurring within reasonable time limits, even when diffusion coefficients are small ($D \approx 10^{-11}$ $cm^2\ sec^{-1}$). Also, ion exchange does not necessarily require defects/nonstoichiometry; stoichiometric solids could exhibit fast exchange of one of its constituents. Following this pioneering work, ion exchange has not only become one of the soft-chemical (*chimie douce*) routes[10] for synthesis of metastable solids that are otherwise inaccessible, but also a convenient and useful technique to probe the mobility of ions through solids in general,[9] particularly lithium ions in metal oxides, providing valuable complementary information in the search for new materials exhibiting fast ion conduction as well as reversible insertion/extraction of lithium. Over the years, we in Bangalore have investigated the mobility of lithium in several oxide systems through ion exchange and ionic conductivity, as well as redox insertion/extraction reactions.

†Based on a lecture delivered at the international symposium "Materials for Energy: Batteries and Fuel Cells", November 2002, Madrid, Spain.

Here, we present an overview of this area, placing our work on metal oxides in the context of international efforts directed at the problem of understanding lithium ion mobility in inorganic solids in general.

2 Rocksalt-related oxides

A large number of oxides of the general formula AMO_2 and A_2MO_3 (A = Li/Na; M = transition metal) crystallize in rocksalt-related superstructures.[11] Among them, α-$NaFeO_2$ is a prototypical structure (Fig. 1) that is adopted by several $LiMO_2$ (M = V, Cr, Co, Ni) oxides.[12] The structure consists of a cubic close-packed (CCP) array of anions, wherein A and M atoms occupy alternate (111) cation planes. Shannon *et al.*[13] were probably the first to report an ion exchange with this structure. They synthesized delafossite (Fig. 2) oxides, $PdMO_2$ and $AgMO_2$ (M = Cr, Co, Rh), from $LiMO_2$ phases *via* the following ion-exchange reactions:

$$2LiMO_2 + Pd + PdCl_2 \rightarrow 2PdMO_2 + 2LiCl$$

$$LiMO_2 + AgNO_3 \rightarrow AgMO_2 + LiNO_3$$

Working with α-$NaCrO_2$ (α-$NaFeO_2$ structure), England *et al.*[8] have shown that facile Na^+/Li^+ as well as Na^+/H^+ exchange occurs in this material topochemically. Subsequently, the work of Poeppelmeier and Kipp[14a] and Dronskowski[14b] on the Li^+/H^+ exchange in $LiAlO_2$ clearly established the role of structure in ion exchange. This oxide crystallizes in three different structures, α, β and γ, of which only the α-form, which has the α-$NaFeO_2$ structure, undergoes Li^+/H^+ exchange in molten benzoic acid. The β- and γ-forms, where both Li and Al are tetrahedrally coordinated (Fig. 3), do not exhibit similar ion exchange. Interestingly, other rocksalt superstructures, for example, α-, β- and γ-$LiFeO_2$, which do not have a layered arrangement of cations,[12] do not show facile ion exchange.

The correlation between ion exchange and redox insertion/extraction of lithium in the α-$NaFeO_2$ structure is clear. Thus, the landmark discovery in 1980[15] of reversible redox extraction/insertion of lithium in $LiCoO_2$ and all the subsequent positive electrode development work[3] for lithium batteries based on this structure appear entirely natural in hindsight, in the light of the high lithium ion mobility in this structure ($D_{300\ K}$ for Li^+ in $LiCoO_2 \approx 5 \times 10^{-9}$ cm^2 sec^{-1}). Motivated by the work of Murphy and co-workers[16] on oxidative deintercalation of Li^+ from $LiVS_2$ using I_2 in CH_3CN, we showed that a similar deintercalation from $LiVO_2$ occurs[17] with Br_2 in $CHCl_3$. Although the material is not suitable as a cathode for lithium batteries for other reasons (*viz.* vanadium atoms migrate to interlayer sites in the deintercalated products),[18] the facile mobility of lithium ions in the α-$NaFeO_2$ structure under both ion-exchange and redox conditions is unmistakable. The fact that ion exchange occurs[8] in α-$NaCrO_2$, but a redox deinsertion of alkali metal ions does not occur with α-$NaCrO_2$/$LiCrO_2$, even with powerful oxidizing agents (*e.g.* Cl_2 in $CHCl_3$), underscores the importance of the redox potential of the transition metal for reversible deinsertion of lithium. On the other hand, Li_2MoO_3, which has a disordered α-$NaFeO_2$ structure,[19] undergoes both Li^+/H^+ exchange and oxidative deinsertion of lithium,[20] again showing that facile ion exchange is an indicator of reversible deinsertion of lithium, provided the redox potential of the accompanying transition metal ion is favorable.

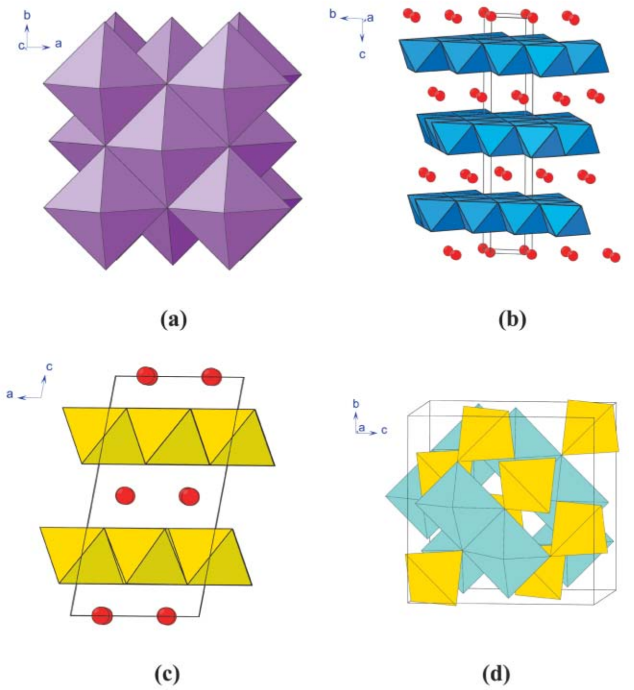

Fig. 1 Structures based on cubic close-packed anion arrays: (a) rocksalt; (b) α-$NaFeO_2$; (c) β-Li_2SnO_3; (d) spinel. In (b) and (c), the red circles denote interlayer alkali metal ions.

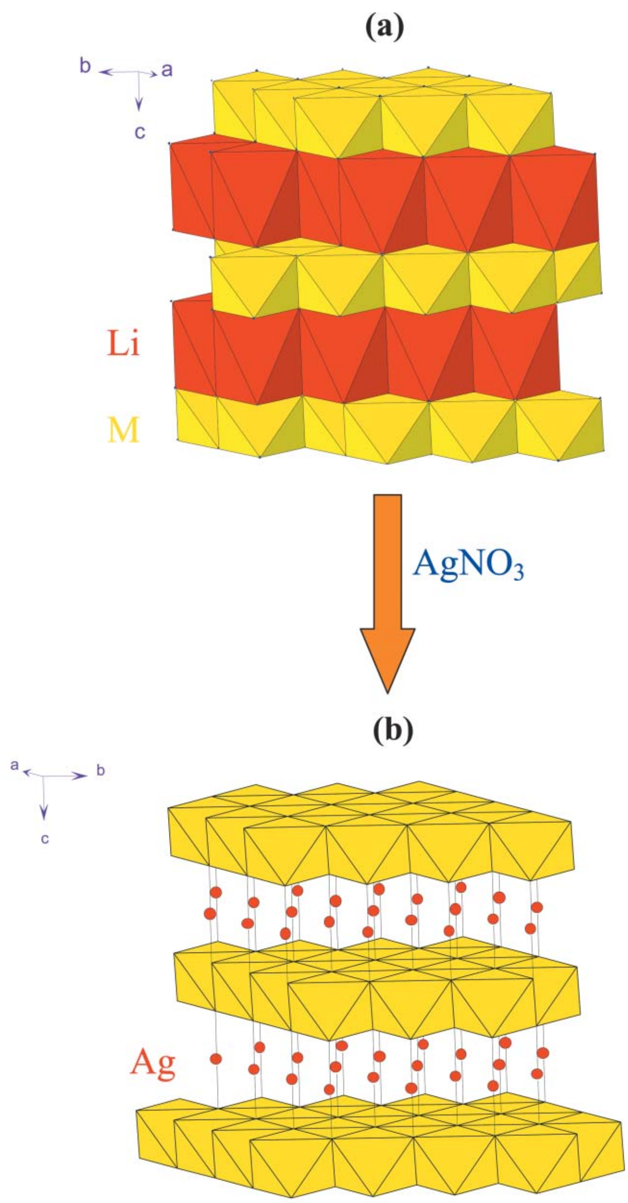

Fig. 2 Transformation of (a) $LiMO_2$ (α-$NaFeO_2$) to (b) $AgMO_2$ (delafossite structure) by ion exchange (M = Cr, Co, Rh).

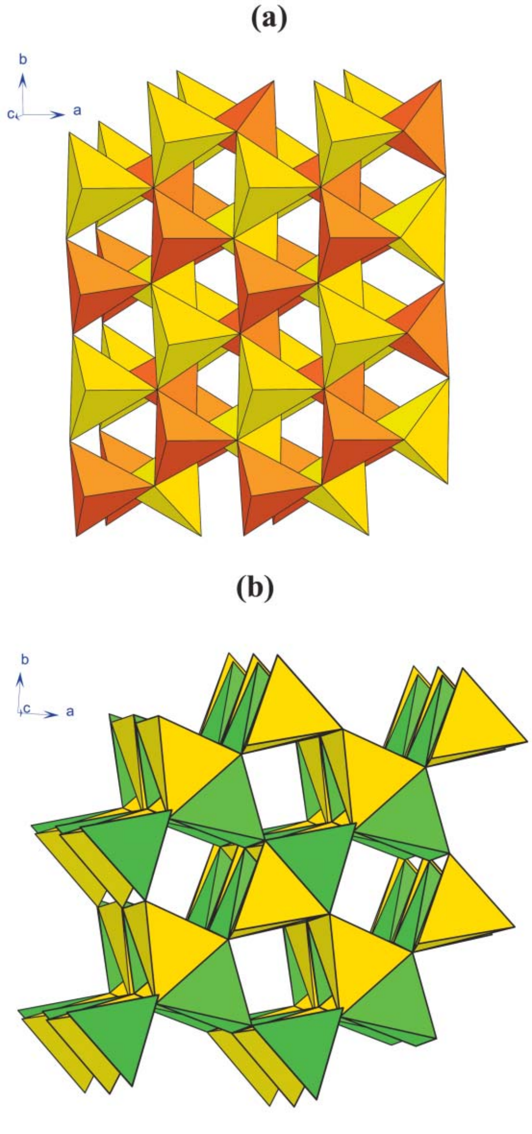

Fig. 3 Structures of (a) β-$LiAlO_2$ and (b) γ-$LiAlO_2$.

Recently we synthesized[21] a new series of oxides of the general formula Li_2MTiO_4 (M^{2+} = Mn, Fe, Co, Ni) that crystallize in cation-disordered rocksalt structures (Fig. 1). For M^{2+} = Ni, we also prepared a low temperature modification that adopts a partially ordered rocksalt structure related to β-Li_2SnO_3. The reluctance of the Li_2MTiO_4 series of oxides to form ordered superstructures even after extended annealing contrasts with the facile ordering of cations in $LiM^{III}O_2$ oxides,[11] and this could be due to the inability to achieve local electroneutrality (Pauling's electroneutrality rule) around oxygens with three different cations, Li^+, M^{2+} and Ti^{4+}, in the rocksalt structure. All the new phases, except M = Ni, undergo oxidative deinsertion of lithium in air/O_2 at elevated temperatures, yielding $LiMTiO_4$ spinels (M = Mn, Fe) and the spinel-like $Li_{1+x}CoTiO_4$ as final products. We believe that Li_2MTiO_4 oxides are attractive candidates for investigation of electrochemical deinsertion of lithium based on the M^{3+}/M^{2+} redox couple.

Although the spinel (AB_2O_4) structure (space group $Fd\bar{3}m$) [Fig. 1(d)] is not exactly a superstructure of rocksalt, it has the same CCP array of anions as in rocksalt. The B_2O_4 framework of edge-shared octahedra (16d and 32e sites) provides an interstitial space of interconnected octahedral (16c) and tetrahedral (8b) empty sites. The empty octahedra and tetrahedra are interconnected with one another through common faces and edges to provide 3D diffusion pathways for Li^+ ion diffusion.[2] Chemical diffusion coefficients are in the range 10^{-8} to 10^{-10} $cm^2\ s^{-1}$. $LiMn_2O_4$ is an archetypal example of a spinel material where a high lithium mobility, both under ion-exchange and redox conditions, has been realized.[2,22] The high lithium mobility under ion exchange conditions was first reported by Hunter,[23] who showed that almost all the lithium in this material could be extracted in aqueous acids (pH ~1–2). The product of acid treatment is, however, not HMn_2O_4, but a new form of manganese(IV) oxide, λ-MnO_2, that retains the spinel framework. Formation of λ-MnO_2 is thought to occur *via* surface disproportionation of Mn^{3+} to Mn^{2+}/Mn^{4+}, the overall chemical reaction being:

$$2LiMn_2O_4 + 4H^+ \rightarrow 2Li^+ + Mn^{2+} + 2H_2O + 3MnO_2$$

Subsequent work[22,24] has shown that complete removal of Li^+ does not occur; Hunter's λ-MnO_2 is actually Li_xMnO_2, where $x \approx 0.02$ in the best leached samples. Reversible deinsertion at 4 V (to give $Li_{1-x}Mn_2O_4$; $0 < x < 1.0$) and insertion at 3 V (to give $Li_{1+y}Mn_2O_4$; $0 < y < 0.8$) renders $LiMn_2O_4$ a unique positive electrode material for lithium battery applications.[2,3] Again the correlation between facile ion exchange and redox insertion/deinsertion of lithium in spinel $LiMn_2O_4$ is indeed unmistakable. More recent work with the oxides of spinel structure has provided a number of electrode materials for lithium batteries:[25–28] $LiMn_{2-x}Al_xO_{4-y}F_y$, $LiMnVO_4$, $LiNiVO_4$, $LiCrMnO_4$, $Li_2FeMn_3O_8$ and $Li[Li_{1/3}Ti_{5/3}]O_4$; the last one inserting a lithium ion at 1.56 V makes it a useful negative electrode material for all-oxide lithium ion cells. Hunter's work on lithium removal from $LiMn_2O_4$ provides a useful indication of the mobility of lithium ions in the spinel structure, and it has been followed up with other lithium-containing spinel oxides.[29,30]

3 Other close-packed oxides

The work of England *et al.*[8] has shown that the Li^+ ion is unique, having a considerable mobility in close-packed oxide lattices, unlike other alkali metal cations, which require more open-channel/layered structures for their mobility. A Li^+ mobility corresponding to $D \approx 10^{-7}$–10^{-8} $cm^2\ s^{-1}$ appears to be common in several close-packed oxides.[8] A dramatic illustration of the high mobility of Li^+ in hexagonal close-packed (HCP) oxide structures is provided by the work of Rice and Jackel[31] on Li^+/H^+ exchange in $LiNbO_3$ and $LiTaO_3$. Both these oxides undergo smooth Li^+/H^+ exchange in hot aqueous acids (for example, 9 M H_2SO_4, 125 °C, 8 h; to give $HNbO_3$ from $LiNbO_3$). What is remarkable about this exchange is that during the reaction, the HCP anion array of $LiMO_3$ (M = Nb, Ta) is transformed into a cubic ReO_3-like array without breaking the M–O bonds (Fig. 4). The mechanism, as was first pointed out by Megaw,[32] involves a simple twisting of the octahedral framework along the hexagonal *c* axis of $LiMO_3$ (the [111] direction for the ReO_3 structure) so as to change the M–O–M bond angle from 157 to 180°. The fact that the same transformation occurs in reverse with ReO_3 on reductive insertion of lithium[33] to give $LiReO_3$ again underscores the close relationship between Li^+/H^+ exchange and redox insertion/deinsertion of lithium. Considering that the anion array of the rutile structure is only slightly distorted from the ideal HCP array,[34] it is not surprising that the trirutile oxides $LiNbWO_6$ and $LiTaWO_6$ also undergo a similar Li^+/H^+ exchange[35] in hot 9–13 M H_2SO_4. Here, the mechanism[36] likely involves transformation of the tetragonal close-packed array of anions of the rutile structure to a HCP array, followed by a rearrangement of cations to give a $LiNbO_3$-like structure for $LiMWO_6$ (M = Nb/Ta) that eventually converts to ReO_3-like $HMWO_6$.

Significantly, $LiSbO_3$, which also has a structure based on a HCP array of anions[37] [Fig. 4(c)] requires a long time (one

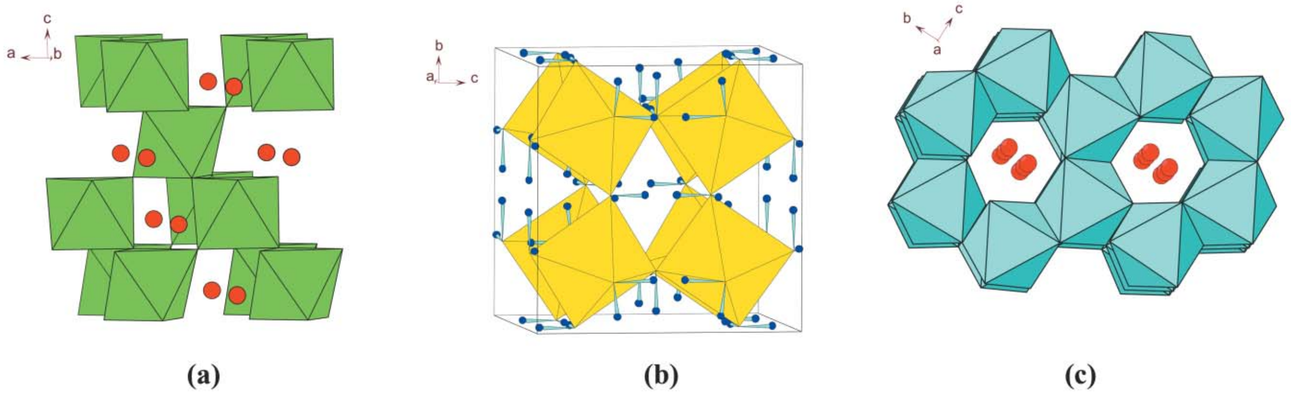

Fig. 4 Structures of (a) $LiNbO_3$, (b) $HNbO_3$ and (c) $LiSbO_3$. In (a) and (c), the red circles within the channels denote Li. In (b), the sticks attached to the corners of the octahedra denote the hydroxyls.

month) for the Li^+/H^+ exchange and the product, $HSbO_3$, retains the parent HCP array.[38] More interestingly, trirutile[39,40] $LiMWO_6$ and the related $LiMMoO_6$ (M = Nb, Ta) undergo a smooth topotactic Li^+/H^+ exchange in dilute (2 M) HNO_3 at room temperature, yielding the novel layered oxides $HMWO_6 \cdot H_2O$ and $HMMoO_6 \cdot H_2O$, which retain the parent rutile structure (Fig. 5). The exchange reveals a fast 2D mobility of Li^+ in this structure, which is supported by diffusion coefficient measurements. The high Li^+ mobility coupled with the strong Brønsted acidity of $HMWO_6$ has been exploited to synthesize polyaniline–$HMWO_6$ nanocomposites that exhibit electrochemical lithium insertion.[41]

$LiFePO_4$, which is a serious candidate for positive electrodes in the next generation of lithium batteries,[1,42] has a HCP array of oxide ions, where Li^+ resides in octahedral sites (Fig. 6). A limitation due to the poor electronic conductivity has been overcome by 'nanopainting' this material with a thin ($\sim$1 nm) coating of carbon.[43] Considering the structure and redox deinsertion of lithium, we expect this material to exhibit facile Li^+/H^+ exchange in aqueous acids yielding novel $HFePO_4$ and $FePO_4$ oxides. LISICONS, $Li_{2+2x}Zn_{1-x}GeO_4$ and $Li_{3+x}(Ge_xV_{1-x})O_4$, containing a HCP array of anions (Fig. 7) exhibit high lithium mobility in ionic conductivity measurements.[5] As compared to the parent oxides, Li_2ZnGeO_4 and Li_3VO_4 (Fig. 7), the best ion-conducting compositions, $Li_{3.5}Zn_{0.25}GeO_4$ and $Li_{3.5}Ge_{0.5}V_{0.5}O_4$ contain supernumerary lithium ions at octahedral sites that give rise to lithium mobility in these materials.[44] Our recent ion-exchange studies[45] have shown that, while no Li^+/H^+ exchange occurs with Li_2ZnGeO_4, the interstitial lithium ions in $Li_{3.5}Zn_{0.25}GeO_4$ (0.75 Li^+ per formula unit) are easily extracted into dilute acids. Redox insertion of lithium into LISICON-related Li_3CrO_4 has been reported.[46]

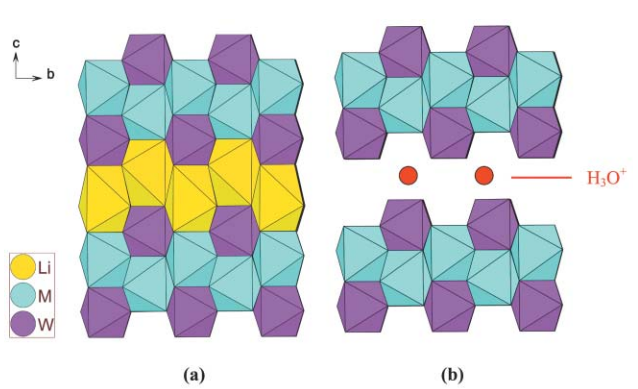

Fig. 5 Transformation of (a) trirutile $LiMWO_6$ (M = Nb, Ta) to (b) layered $HMWO_6 \cdot H_2O$ by Li^+/H^+ exchange.

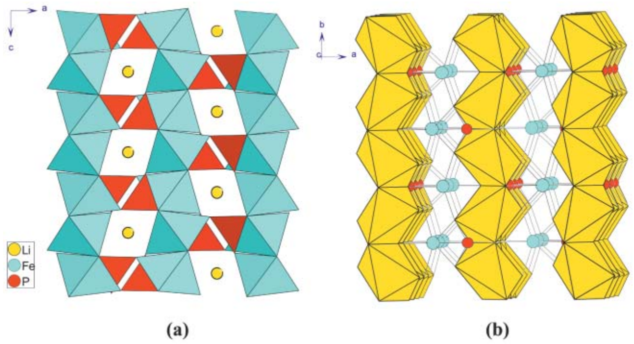

Fig. 6 Structure of $LiFePO_4$ showing (a) corner-sharing FeO_6 octahedral layers and (b) edge-sharing LiO_6 octahedral chains.

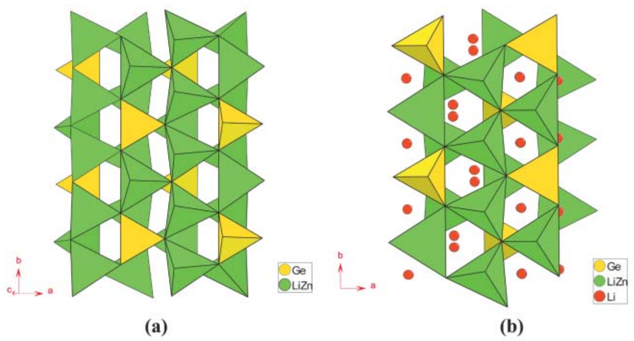

Fig. 7 Structures of (a) Li_2ZnGeO_4 and (b) $Li_{3.5}Zn_{0.25}GeO_4$ (LISICON). In (b), the red circles within the channels denote interstitial Li^+ ions.

4 Perovskite oxides

Layered perovskite oxides of the Ruddlesden–Popper type, $NaLaTiO_4$ and $K_2La_2Ti_3O_{10}$, undergo ready Na^+/Li^+ and K^+/Li^+ exchange[47,48] in molten $LiNO_3$, giving the lithium analogs $LiLaTiO_4$ and $Li_2La_2Ti_3O_{10}$. In the exchanged products, Li^+ is tetrahedrally coordinated, unlike the parent materials, wherein Na^+/K^+ has a nine-fold (monocapped square antiprism) oxygen coordination (Fig. 8). The Li^+-exchanged layered perovskites exhibit poor lithium mobility, as revealed by the low lithium ion conductivity of these materials.[47] On the other hand, a 3D perovskite phase in the (Li, La)TiO_3 system, first reported by Belous *et al.*,[49] exhibits a bulk ionic conductivity of $\sim 1 \times 10^{-3}$ S cm^{-1} at room temperature.[50] This remarkable result has triggered off a great deal of research activity on these materials in recent times.[51] The structure of the Li^+ ion-conducting perovskite phase[52] in the (Li, La)TiO_3 system is rather unusual in that the Li^+ which is normally expected to

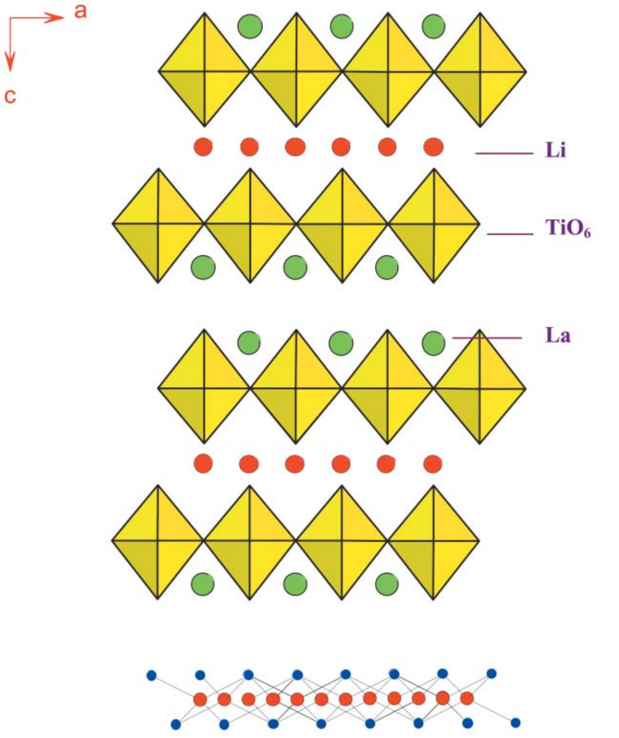

Fig. 8 Structure of $LiLaTiO_4$. The tetrahedral oxygen (blue) coordination around Li is shown separately at the bottom.

occupy the B site on the basis of size considerations, goes to a special (18d) site in the $R\bar{3}c$ structure, which is at the center of the oxygen windows formed by four TiO_6 octahedra [Fig. 9(a)]. The partially occupied Li and La sites in this structure provide an interconnected pathway for the migration of lithium, involving 5/6 of the unoccupied 18d sites, as well as 1/2 of the 6a sites. The high mobility of Li^+ in $(Li,La)TiO_3$ is evidenced by the facile Li^+/H^+ exchange[53] in 2 M HNO_3 at 60 °C.

A major problem with the possible use of this material as an electrolyte in lithium batteries is the reduction[51a] of Ti^{4+} to Ti^{3+} at relatively low potentials (~2 V), with the onset of electronic conductivity and short circuiting. We believed that it should be possible to design perovskite-type lithium ion conductors that retain the attractive features of $(Li, La)TiO_3$, but eliminate the reduction problem by a suitable choice of A and B atoms. In an effort to understand the factors that control lithium ion conduction in perovskite oxides, we synthesized[54] several stoichiometric perovskite oxides of the formulas

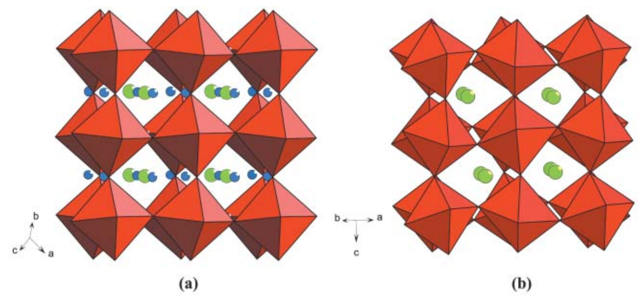

Fig. 9 Structures of perovskite lithium ion conductors: (a) $(Li, La)TiO_3$; (b) $LiCa_{1.65}\square_{0.35}Ti_{1.3}Nb_{1.7}O_9$. In (a), the green and blue circles denote La and Li, respectively. In (b), the green circles denote Li and Ca in the $GdFeO_3$ structure.

$LiABB'O_6$ and $LiA_2B_2B'O_9$ in Li–A–B–B′–O (A = Ca, Sr, Ba; B = Ti, Zr; B′ = Nb, Ta) systems and investigated their structures and lithium ion conductivity. Our results, which are summarized in Table 1 and Fig. 10, suggest: (i) conductivity increases with increasing pentavalent metal, as can be seen from a comparison of the data for $LiSrTiNbO_6$ and $LiSr_2Ti_2NbO_9$; (ii) for oxides of the same generic formula, the B′ = Ta compounds exhibit a higher conductivity than the corresponding B′ = Nb compounds; this can be seen by comparing the conductivity data for the pairs of oxides $LiSrTiNbO_6/LiSrTiTaO_6$ and $LiSr_2Ti_2NbO_9/LiSr_2Ti_2TaO_9$; (iii) for oxides of the same formula, the strontium compounds exhibit a higher conductivity than the corresponding calcium or barium compounds. This conclusion is based on the data for $LiA_2Ti_2NbO_9$ (A = Ca, Sr, Ba). Similar correlations between chemical composition and lithium ion conductivity in $(Li,La)TiO_3$ and $(Li,Ln)TiO_3$ (Ln = rare earth) have been reported in the literature.[50] The A-site vacancy concentration is another crucial factor that determines lithium ion conductivity.[55] The best ionic conduction is obtained when the total concentration of lithium and A-site vacancies is 0.44–0.45.

We arrived at the composition $LiSr_{1.65}\square_{0.35}B_{1.3}B'_{1.7}O_9$ (B = Ti; B′ = Nb, Ta; **I**), which optimizes all the above factors. Thus, we chose Sr in preference to Ca or Ba for the A site because Sr provides optimal 'bottleneck' size for Li^+ migration, the Sr content (0.55) per ABO_3 formula unit being the same as the La content of the best lithium ion-conducting composition in the $(Li,La)TiO_3$ system. Composition **I** also has a significant concentration of pentavalent (Nb/Ta) ions at the B site, which is known to promote Li^+ conduction by weakening Li–O bonds.

Cubic perovskite oxides of composition **I** were readily obtained[54] by solid-state reaction of the constituent oxides at 1200 °C, followed by quenching. Of the Nb/Ta phases, the Ta

Table 1 Chemical composition, lattice parameters and lithium ion-conductivity data for perovskite oxides in the Li–A–B–B′–O (A = Ca, Sr, Ba; B = Ti, Zr; B′ = Nb, Ta) systems

Composition[a]	Synthesis conditions: temperature/°C (duration/h)	Lattice parameter/Å	$\sigma_{30\ °C}$/S cm^{-1}	$\sigma_{360\ °C}$/S cm^{-1}	E_a/eV
$LiCaTiNbO_6$	800 (12), 1150 (12 + 12), 1200 (12)	—[b]	$<10^{-7}$	6.3×10^{-6}	0.68 (200–700 °C)
$LiSrTiNbO_6$	800 (12), 1150 (12 + 12), 1250 (18)	3.932(1)	$<10^{-6}$	8.9×10^{-4}	0.42
$LiSrTiTaO_6$[c]	800 (12), 1100 (10), 1350–1400 (4–6)	3.932	5.5×10^{-4}	6.3×10^{-2}	0.33
$LiCa_2Ti_2NbO_9$	800 (12), 1150 (12 + 12), 1200 (24)	—[d]	$<10^{-8}$	7.1×10^{-7}	1.03 (300–700 °C)
$LiSr_2Ti_2NbO_9$	800 (12), 1150 (12 + 12), 1200 (12)	3.924(2)	$<10^{-6}$	3.2×10^{-4}	0.34
$LiBa_2Ti_2NbO_9$	800 (12), 1150 (12 + 12), 1200 (12)	4.031(1)	$<10^{-7}$	2.0×10^{-5}	0.74 (200–700 °C)
$LiSr_2Ti_2TaO_9$[e]	1100 (12), 1250 (9)	3.925(1)	3.2×10^{-5}	3.2×10^{-3}	0.27
$LiSr_{1.65}\square_{0.35}Ti_{1.3}Nb_{1.7}O_9$[e]	1100 (12), 1200 (6)	3.932(1)	2.0×10^{-5}	4.2×10^{-2}	0.34[f]
$LiSr_{1.65}\square_{0.35}Ti_{1.3}Ta_{1.7}O_9$[e]	1100 (12), 1250 (6)	3.932(1)	4.9×10^{-5}	0.114	0.35[f]
$LiSr_{1.65}\square_{0.35}Zr_{1.3}Ta_{1.7}O_9$[e]	1100 (12), 1300 (9)	4.017(1)	1.3×10^{-5}	0.125	0.36[f]
$Li_{0.36}La_{0.55}\square_{0.09}TiO_3$[g]	650 (2), 800 (12), 1350 (1)	3.8710(2)	2.0×10^{-5}	0.130	0.33

[a]Excess (10 mol%) Li_2CO_3 was added to compensate for the loss of lithium at high temperature. [b]Orthorhombic: a = 5.365(2), b = 5.486(2), c = 7.666(3) Å. [c]Data taken from ref. 50d. [d]Orthorhombic: a = 5.374(3), b = 5.487(3), c = 7.674(1) Å. [e]Samples were quenched to room temperature at the last stage. [f]Activation energies were obtained form the conductivity data in the temperature range 30–200 °C. [g]For comparison, the data[50a] for cubic $Li_{0.36}La_{0.55}\square_{0.09}TiO_3$ are included.

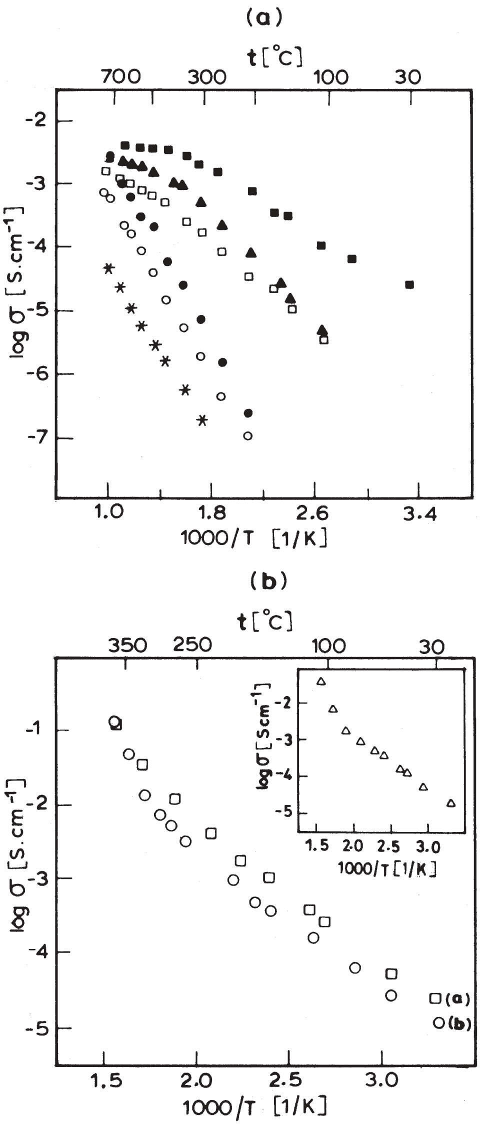

Fig. 10 (a) Arrhenius plots for the ionic conductivity of $LiABB'O_6$ and $LiA_2B_2B'O_9$ perovskites: $LiCaTiNbO_6$ (○), $LiSrTiNbO_6$ (▲), $LiCa_2Ti_2NbO_9$ (*), $LiSr_2Ti_2NbO_9$ (□), $LiBa_2Ti_2NbO_9$ (●) and $LiSr_2Ti_2TaO_9$ (■). (b) Arrhenius plots for the conductivity of $LiSr_{1.65}\square_{0.35}Ti_{1.3}Ta_{1.7}O_9$ (□) and $LiSr_{1.65}\square_{0.35}Zr_{1.3}Ta_{1.7}O_9$ (○). The data for $LiSr_{1.65}\square_{0.35}Ti_{1.3}Nb_{1.7}O_9$ are shown in the inset. (After ref. 54.)

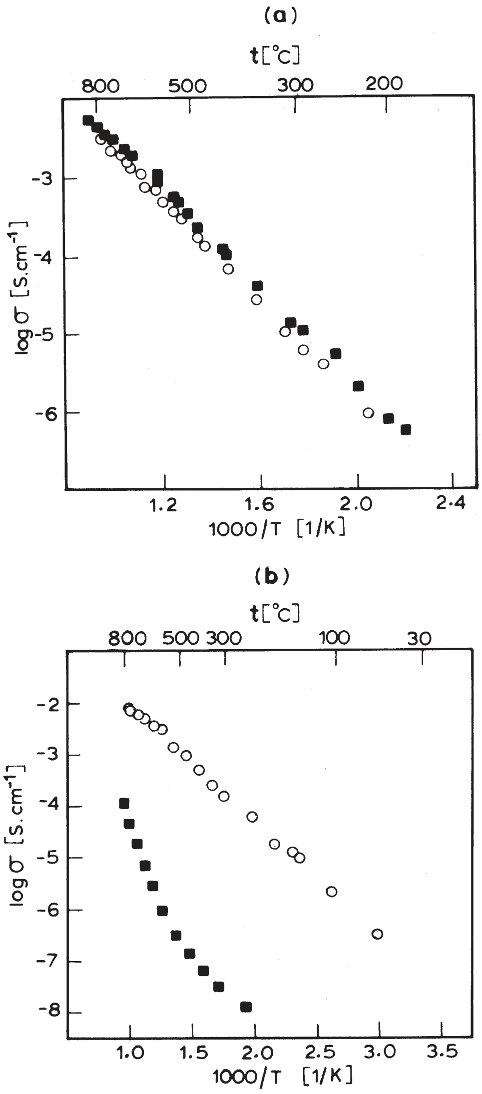

Fig. 11 (a) Arrhenius plots for the ionic conductivity of $LiCa_{1.65}\square_{0.35}Ti_{1.3}Nb_{1.7}O_9$ (○) and $LiCa_{1.65}\square_{0.35}Ti_{1.3}Ta_{1.7}O_9$ (■). (b) Arrhenius plots for the ionic conductivity of $LiSr_{1.65}\square_{0.35}Ti_{2.15}W_{0.85}O_9$ (○) and $LiSr_2Ti_{2.5}W_{0.5}O_9$ (■). (After ref. 56.)

phase exhibited a higher ionic conductivity, as expected [Fig. 10(b)]. The conductivity of this phase is comparable to the best conducting phase in the (Li,La)TiO_3 system. Having obtained one of the best lithium ion conductors by a rational choice of chemical composition, next we attempted to prepare a lithium ion conductor that would not suffer a reduction of B-site ions when coming into contact with lithium metal. For this purpose, we chose the composition $LiSr_{1.65}\square_{0.35}Zr_{1.3}Ta_{1.7}O_9$ (**II**), where Zr^{4+} replaces Ti^{4+}. A single-phase perovskite oxide (a = 4.017 Å) for this composition was obtained by reacting the constituents at 1300 °C, followed by quenching. We believe this oxide, exhibiting a low conductivity of 1.3×10^{-5} S cm^{-1} at 30 °C, but a high conductivity of ~0.1 S cm^{-1} at 400 °C should be a candidate electrolyte for high temperature solid-state lithium battery applications. Moreover, the material also contains stable oxidation states, Zr^{4+} and Ta^{5+}, that do not undergo a reduction at a lithium anode.

In an attempt to probe further the influence of A-site ions on the conductivity of phases **I**, we investigated[56] similar compositions containing Ca instead of Sr: $LiCa_{1.65}\square_{0.35}Ti_{1.3}B'_{1.7}O_9$ (B′ = Nb, Ta; **III**). Phases **III** have orthorhombic ($GdFeO_3$) structures [Fig. 9(b) and Table 2] and exhibit lower

Table 2 Chemical composition, lattice parameters and lithium ion-conductivity data for perovskite oxides in the Li–Ca–Ti–Nb/Ta–O and Li–Sr–Ti–W–O systems

Composition	Synthesis conditions: temperature/°C (duration/h)	Lattice parameter/Å	$\sigma_{300\ °C}$/S cm^{-1}	$\sigma_{800\ °C}$/S cm^{-1}	E_a/eV
$LiCa_{1.65}\square_{0.35}Ti_{1.3}Nb_{1.7}O_9$	1100 (12), 1200 (6), 1250 (6)	—[a]	1.0×10^{-5}	3.1×10^{-3}	0.71
$LiCa_{1.65}\square_{0.35}Ti_{1.3}Ta_{1.7}O_9$	1100 (12), 1200 (6), 1250 (6)	—[b]	1.0×10^{-5}	4.2×10^{-3}	0.68
$LiSr_2Ti_{2.5}W_{0.5}O_9$	1200 (12 + 12)	3.925(1)	1.1×10^{-7}	1.0×10^{-4}	1.30
$LiSr_{1.65}\square_{0.35}Ti_{2.15}W_{0.85}O_9$	1200 (12 + 12)	3.911(1)	1.6×10^{-4}	9.4×10^{-3}	0.49

[a]Orthorhombic: a = 5.363(1), b = 5.464(1), c = 7.662(3) Å. [b]Orthorhombic: a = 5.363(1), b = 5.456(1), c = 7.661(1) Å.

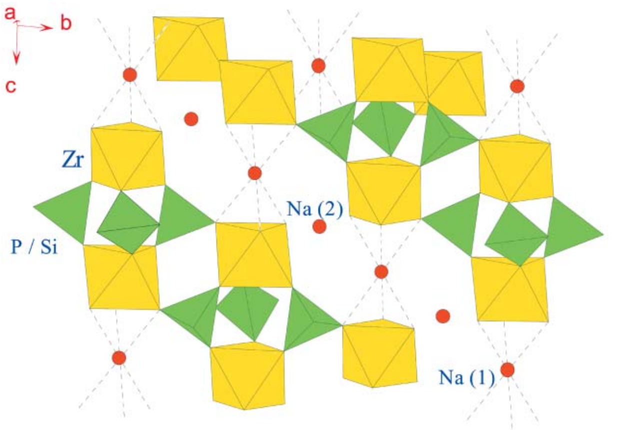

Fig. 12 Structure of $Na_3Zr_2PSi_2O_{12}$ (NASICON). The red circles denote Na (1) and Na (2) occupying the interconnected channels within the framework.

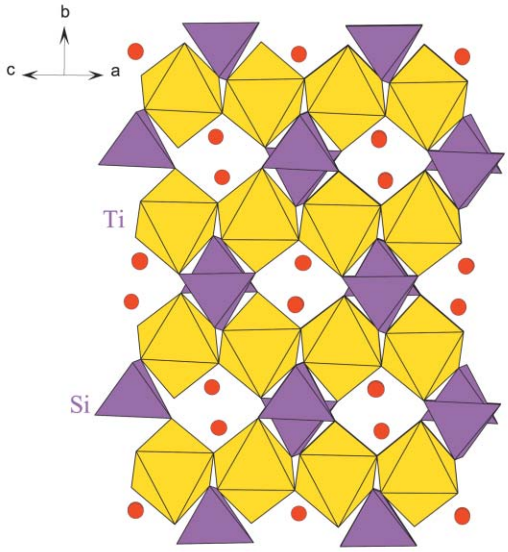

Fig. 13 Structure of $CaTiOSiO_4$ (titanite). The red circles within the channels denote Ca.

ionic conductivity [Fig. 11(a)] than the Sr analogs. Interestingly, we were also able to prepare[56] Ti^{4+}/W^{6+} analogs of **I**, $LiSr_{1.65}\square_{0.35}Ti_{2.15}W_{0.8}O_9$ (**IV**) and its stoichiometric parent, $LiSr_2Ti_{2.5}W_{0.5}O_9$ (**V**). Although **IV** has a much higher conductivity than the parent phase [Fig. 11(b)], its conductivity is considerably lower than that of the Ti/Nb and Ti/Ta analogs (**I**). The Ti^{4+}/W^{6+} combination at the B sites in **IV** presumably creates a more unsymmetrical potential energy profile for the migration of Li^+ than the Ti^{4+}/Nb^{5+} and Ti^{4+}/Ta^{5+} combinations in **I**, impeding the mobility of lithium in **IV**.

5 Framework oxides

NASICON ($Na_3Zr_2PSi_2O_{12}$) is a well-known framework oxide (Fig. 12) that exhibits fast sodium ion conduction[57] as well as sodium ion exchange.[9] Na^+/Li^+ exchange in NASICON was reported by Hong in his pioneering work[58] on framework oxides. Sometime back, we showed[59] that the substitution $2Zr^{2+} \rightarrow M^{5+} + M^{3+}$ in NASICON is possible, yielding several new mixed metal phosphates of the general formula $AM^{5+}M^{3+}(PO_4)_3$ (A = Na, Li; M^{5+} = Nb, Ta; M^{3+} = Ti, V, Cr, Fe, Al). An investigation of the ionic conductivity of lithium derivatives[60] has shown that $LiTaAl(PO_4)_3$ exhibits the highest conductivity, $\sigma \approx 1 \times 10^{-2}$ S cm^{-1} (E_a = 0.47 eV), comparable to the conductivity of $LiTi_2(PO_4)_3$. Recent interest in this structure has focused on developing cathode materials for lithium batteries. The redox mobility of Na^+ in the NASICON framework was reported by our group[61] in $Na_3V_2(PO_4)_3$. We have showed that Na^+ can be oxidatively removed from $Na_3V_2(PO_4)_3$ using Cl_2 in non-aqueous solvents. The oxidized products, $Na_{3-x}V_2(PO_4)_3$ ($0 < x < 3$) retained the NASICON framework of $V_2(PO_4)_3$. More recently, Goodenough *et al.*[62] have investigated electrochemical insertion/deinsertion of lithium in several NASICON framework materials containing V^{4+}/V^{3+}, Fe^{3+}/Fe^{2+}, Ti^{4+}/Ti^{3+}, among others, and the work has led to the discovery of a new 3.7 V lithium insertion cathode material,[63] *viz.* $Li_2NaV_2(PO_4)_3$, having the rhombohedral NASICON framework. The related[64] $Li_3V_2(PO_4)_3$ also deinserts two lithium ions at 3.77 V. Significantly, both $Li_2NaV_2(PO_4)_3$ and $Li_3V_2(PO_4)_3$ have been prepared by ion exchange in aqueous $LiNO_3$ starting from $Na_3V_2(PO_4)_3$. The NASICON framework is indeed unique in that it exhibits all three properties, *viz.* ionic conductivity, ion exchange and redox insertion/extraction, that characterize lithium ion mobility in ionic solids.

Titanite/sphene ($CaTiOSiO_4$) is a framework structure (Fig. 13) consisting of TiO_6 octahedra and SiO_4 tetrahedra,[65] where the extra-framework cations are located in the channels. A number of lithium-containing analogs are known wherein one would expect Li^+ ion mobility.[66] Li^+ ion conductivity has been investigated[67] in $LiMn(OH)PO_4$ and $LiMn(OH)AsO_4$. Although both the materials are topologically related[68] (Fig. 14), the location of Li^+ ions is different. In $LiMn(OH)AsO_4$, the MnO_6 octahedra are linked *via* opposite vertices by OH^- groups to form infinite zigzag chains in the [101] direction that are interconnected by AsO_4 tetrahedra. Li^+ ions reside in the enclosed channels that run in the [001] direction. In the $LiMn(OH)PO_4$ structure, the MnO_6 octahedra are also

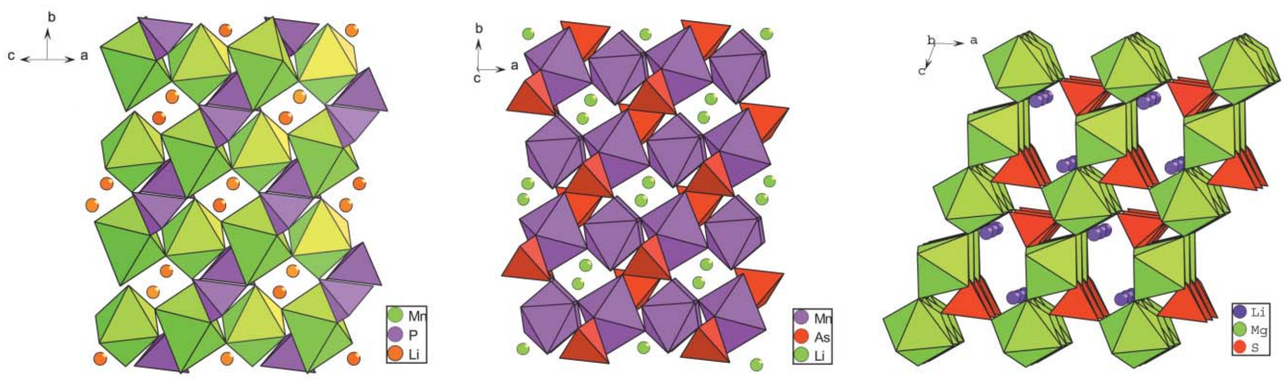

(a) **(b)** **(c)**

Fig. 14 Structures of (a) $LiMnPO_4(OH)$, (b) $LiMnAsO_4(OH)$ and (c) $LiMgFSO_4$. The filled circles within the channels denote Li.

linked through opposite vertices by OH^- groups to give infinite zigzag chains that lie in the [001] direction. Li^+ ions are located in the channels that run in the [101] direction. The phosphate is a better Li^+ ion conductor[67] ($\sigma_{200\ °C} = 3 \times 10^{-5}$ S cm^{-1}) than the arsenate ($\sigma_{200\ °C} = 1 \times 10^{-9}$ S cm^{-1}) and the difference has been attributed to wider channels in the phosphate that allow greater lithium mobility. We prepared a new sphene derivative, $LiFMgSO_4$ [Fig. 14(c)], where Li^+ is located in two half-occupied sites.[66] The Li^+ conductivity of this material is intermediate between the conductivities of $LiMn(OH)XO_4$ (X = P, As). Our work on $LiMgFSO_4$ was motivated by a desire to prepare transition metal derivatives, $LiMFSO_4$ (M = 3d metal), which could be interesting materials to explore redox deinsertion of lithium based on the M^{3+}/M^{2+} redox couple. This objective, however, remains to be realized.

Conclusion

In this brief survey of metal oxides containing mobile lithium, we have made an attempt to provide a chemical perspective on the topic, bringing out the relationships between crystal structure and properties associated with mobile lithium. Ionic conductivity, redox insertion/deinsertion and ion exchange are the common measurable properties that depend on lithium ion mobility. Among them, ion exchange is a convenient property to study, and gives valuable information on lithium mobility. While facile lithium ion exchange does not automatically guarantee a high ionic conductivity or redox insertion/deinsertion of lithium, it provides useful insights into structure and bonding requirement for high lithium mobility in a solid. Thus, high lithium mobility is found in both close-packed and open-framework structures. Within the close-packed structures, specific cation orderings seem to favor high mobility. For example, among the several rocksalt-based oxide superstructures, the α-$NaFeO_2$ structure, consisting of alternate (111) layers of monovalent and trivalent cations in a CCP anion array, appears to be the most favored arrangement for high lithium mobility, both under ion-exchange (*e.g.* α-$LiAlO_2$) and redox conditions (*e.g.* $LiCoO_2$). The spinel structure, containing an interconnected interstitial space of empty octahedral and tetrahedral sites, is another close-packed structure where high lithium mobility, both under ion-exchange and redox conditions, is found, as revealed by the work on $LiMn_2O_4$ and related spinel oxides. Among the HCP-related structures, both $LiNbO_3/LiTaO_3$ and ordered trirutile phases, such as $LiNbWO_6$, exhibit high lithium mobility, although the related $LiSbO_3$ and $LiSbWO_6$ show poor mobility, as revealed by Li^+/H^+ exchange experiments, highlighting the effect of the difference in bonding between d^{10} Sb^{5+} and d^0 Nb^{5+}/Ta^{5+} on lithium mobility. Redox lithium mobility in the HCP-based olivine oxide $LiFePO_4$ makes it an attractive positive material for the next generation of lithium batteries. The high lithium mobility in the HCP-based LISICON oxides in ionic conductivity and ion-exchange studies suggests the possibility of developing new positive electrode materials based on this structure. The perovskite structure also favors high lithium mobility, as exemplified by $(Li,La)TiO_3$ and our recent work on $LiA_{1.65}\square_{0.35}B_{1.3}B'_{1.7}O_9$ (A = Sr, Ca; B = Ti, Zr; B′ = Nb, Ta), but further work is required to understand the factors involved. Among the framework oxides, NASICON ($Na_3Zr_2PSi_2O_{12}$) remains unique as a structure that supports high lithium mobility under ion-exchange, ionic conductivity and redox insertion/deinsertion experiments. We hope that this survey will prove useful in the ongoing search for new materials exhibiting high lithium ion mobility for battery applications.

Acknowledgements

We thank the Department of Science and Technology, Government of India, and the Council of Scientific and Industrial Research (CSIR), New Delhi, for financial support. L. S. thanks CSIR for the award of a research fellowship. Our thanks are also due to Professor A. K. Shukla for collaboration in ionic conductivity studies.

References

1 (*a*) *MRS Bull.*, 2002, **27**(8); (*b*) J.-M. Tarascon and M. Armand, *Nature*, 2001, **414**, 359; (*c*) M. Wakihara, *Mater. Sci. Eng., R*, 2001, **33**, 109.
2 (*a*) M. Winter, J. O. Besenhard, M. E. Spahr and P. Novák, *Adv. Mater.*, 1998, **10**, 725; (*b*) M. Broussely, P. Biensan and B. Simon, *Electrochim. Acta*, 1999, **45**, 3.
3 D. Guyomard, in *New Trends in Electrochemical Technology: Energy Storage Systems in Electronics*, ed. T. Osaka and M. Datta, Gordon and Breach Publishers, Philadelphia, 2000, ch. 9.
4 G. Adachi, N. Imanaka and H. Aono, *Adv. Mater.*, 1996, **8**, 127.
5 A. D. Robertson, A. R. West and A. D. Ritchie, *Solid State Ionics*, 1997, **104**, 1.
6 (*a*) J. Alper, *Science*, 2002, **296**, 1224; (*b*) F. Croce, G. B. Appetecchi, L. Persi and B. Scrosati, *Nature*, 1998, **394**, 456.
7 *Solid State Electrochemistry*, ed. P. G. Bruce, Cambridge University Press, Cambridge, 1995.
8 W. A. England, J. B. Goodenough and P. J. Wiseman, *J. Solid State Chem.*, 1983, **49**, 289.
9 A. Clearfield, *Chem. Rev.*, 1988, **88**, 125.
10 (*a*) J. Gopalakrishnan, *Chem. Mater.*, 1995, **7**, 1265; (*b*) R. E. Schaak and T. E. Mallouk, *Chem. Mater.*, 2002, **114**, 1455.
11 G. C. Mather, C. Dussarrat, J. Etourneau and A. R. West, *J. Mater. Chem.*, 2000, **10**, 2219.
12 T. A. Hewston and B. L. Chamberland, *J. Phys. Chem. Solids*, 1987, **48**, 97.
13 R. D. Shannon, D. B. Rogers and C. T. Prewitt, *Inorg. Chem.*, 1971, **10**, 713.
14 (*a*) K. R. Poeppelmeier and D. O. Kipp, *Inorg. Chem.*, 1988, **27**, 766; (*b*) R. Dronskowski, *Inorg. Chem.*, 1993, **32**, 1.
15 K. Mizushima, P. C. Jones, P. J. Wiseman and J. B. Goodenough, *Mater. Res. Bull.*, 1980, **15**, 783.
16 (*a*) D. W. Murphy, C. Cros, F. J. Di Salvo and J. V. Waszczak, *Inorg. Chem.*, 1977, **16**, 3027; (*b*) D. W. Murphy, J. N. Carides, F. J. DiSalvo, C. Cros and J. V. Waszczak, *Mater. Res. Bull.*, 1977, **12**, 825.
17 K. Vidyasagar and J. Gopalakrishnan, *J. Solid State Chem.*, 1982, **42**, 217.
18 L. A. de Picciotto, M. M. Thackeray, W. I. F. David, P. G. Bruce and J. B. Goodenough, *Mater. Res. Bull.*, 1984, **19**, 1497.
19 A. C. W. P. James and J. B. Goodenough, *J. Solid State Chem.*, 1988, **76**, 87.
20 J. Gopalakrishnan and V. Bhat, *Mater. Res. Bull.*, 1987, **22**, 769.
21 L. Sebastian and J. Gopalakrishnan, *J. Solid State Chem.*, 2003, in press.
22 J. B. Goodenough, M. M. Thackeray, W. I. F. David and P. G. Bruce, *Rev. Chim. Miner.*, 1984, **21**, 435.
23 J. C. Hunter, *J. Solid State Chem.*, 1981, **39**, 142.
24 A. Mosbah, A. Verbaere and M. Tournoux, *Mater. Res. Bull.*, 1983, **18**, 1375.
25 G. G. Amatucci, N. Pereira, T. Zheng and J.-M. Tarascon, *J. Electrochem. Soc.*, 2001, **148**, A171.
26 A. K. Padhi, W. B. Archibald, K. S. Nanjundaswamy and J. B. Goodenough, *J. Solid State Chem.*, 1997, **128**, 267.
27 G. T.-K. Fey, W. Li and J. R. Dahn, *J. Electrochem. Soc.*, 1994, **141**, 2279.
28 (*a*) T. Ohzuku, A. Ueda and N. Yamomoto, *J. Electrochem. Soc.*, 1995, **142**, 1431; (*b*) S. Kano and M. Sato, *Solid State Ionics*, 1995, **79**, 215; (*c*) G. X. Wang, D. H. Bradhurst, S. X. Dou and H. K. Liu, *J. Power Sources*, 1999, **83**, 156; (*d*) H. Kawai, M. Nagata, M. Tabuchi, H. Tukamoto and A. R. West, *Chem. Mater.*, 1998, **10**, 3226.
29 (*a*) B. Krutzsch and S. Kemmler-Sack, *J. Less-Common. Met.*, 1986, **124**, 111; (*b*) R. Chitrakar, H. Kanoh, Y. Makita, Y. Miyai and K. Ooi, *J. Mater. Chem.*, 2000, **10**, 2325.

30 Y.-F. Liu, Q. Feng and K. Ooi, *J. Solid State Chem.*, 1994, **163**, 130.
31 C. E. Rice and J. L. Jackel, *J. Solid State Chem.*, 1982, **41**, 308.
32 H. D. Megaw, *Ferroelectricity in Crystals*, Methuen, London, 1957, p. 105.
33 R. J. Cava, A. Santoro, D. W. Murphy, S. Zahurak and R. S. Roth, *J. Solid State Chem.*, 1982, **42**, 251.
34 A. F. Wells, *Structural Inorganic Chemistry*, Clarendon Press, Oxford, 5th edn., 1984, pp. 168–169.
35 V. Bhat and J. Gopalakrishnan, *J. Solid State Chem.*, 1986, **63**, 278.
36 J. Gopalakrishnan, *Bull. Mater. Sci.*, 1985, **7**, 201.
37 J. B. Goodenough and J. A. Kafalas, *J. Solid State Chem.*, 1973, **6**, 493.
38 (*a*) R. Chitrakar and M. Abe, *Mater. Res. Bull.*, 1988, **23**, 1231; (*b*) J. L. Fourquet, P. A. Gillet and A. Le Bail, *Mater. Res. Bull.*, 1989, **24**, 1207.
39 V. Bhat and J. Gopalakrishnan, *Solid State Ionics*, 1988, **26**, 25.
40 N. S. P. Bhuvanesh and J. Gopalakrishnan, *Inorg. Chem.*, 1995, **34**, 3760.
41 B. E. Koene and L. F. Nazar, *Solid State Ionics*, 1996, **89**, 147.
42 A. K. Padhi, K. S. Nanjundaswamy and J. B. Goodenough, *J. Electrochem. Soc.*, 1997, **144**, 1188.
43 M. Armand, in *Abstracts of the Materials for Energy: Batteries and Fuel Cells International Symposium, November 4–5, 2002, Madrid, Spain*, Fundación Ramón Areces, Madrid, 2002.
44 P. G. Bruce and I. Abrahams, *J. Solid State Chem.*, 1991, **95**, 74.
45 L. Sebastian, R. S. Jayashree and J. Gopalakrishnan, manuscript in preparation.
46 S. Garcia-Martin, A. D. Robertson, M. A. K. L. Dissanayake and A. R. West, *Solid State Ionics*, 1995, **76**, 309.
47 V. Thangadurai, A. K Shukla, J. Gopalakrishnan, O. Joubert, L. Brohan and M. Tournoux, *Mater. Sci. Forum*, 2000, **321–324**, 965.
48 K. Toda, J. Watanabe and M. Sato, *Mater. Res. Bull.*, 1996, **31**, 1427.
49 A. G. Belous, G. N. Novitskaya, S. V. Polyanetskaya and Yu. I. Gornikov, *Izv. Akad. Nauk SSSR, Neorg. Mater.*, 1987, **23**, 470.
50 (*a*) Y. Inaguma, C. Liquan, L. Chen, M. Itoh, T. Nakamura, T. Uchida, H. Ikuta and M. Wakihara, *Solid State Commun.*, 1993, **86**, 689; (*b*) M. Itoh, Y. Inaguma, W.-H. Jung, L. Chen and T. Nakamura, *Solid State Ionics*, 1994, **70**(71), 203; (*c*) Y. Inaguma, L. Chen, M. Itoh and T. Nakamura, *Solid State Ionics*, 1994, **70**(71), 196; (*d*) Y. Inaguma, Y. Matsui, Y.-J. Shan, M. Itoh and T. Nakamura, *Solid State Ionics*, 1995, **79**, 91.
51 See, for example: (*a*) A. Morata-Orrantia, S. García-Martín, E. Morán and M. A. Alario-Franco, *Chem. Mater.*, 2002, **14**, 2871; (*b*) T. Katsumata, Y. Inaguma, M. Itoh and K. Kawamura, *Chem. Mater.*, 2002, **14**, 3930; (*c*) D. Mazza, S. Ronchetti, O. Bohnké, H. Duroy and J. L. Fourquet, *Solid State Ionics*, 2002, **149**, 81.
52 J. A. Alonso, J. Sanz, J. Santamaría, C. León, A. Várez and M. T. Fernández-Díaz, *Angew. Chem., Int. Ed.*, 2000, **39**, 619.
53 N. S. P. Bhuvanesh, O. Bohnké, H. Duroy, M. P. Crosnier-Lopez, J. Emery and J. L. Fourquet, *Mater. Res. Bull.*, 1998, **33**, 1681.
54 V. Thangadurai, A. K. Shukla and J. Gopalakrishnan, *Chem. Mater.*, 1999, **11**, 835.
55 (*a*) J. L. Fourquet, H. Duroy and M. P. Crosnier-Lopez, *J. Solid State Chem.*, 1996, **127**, 283; (*b*) Y. Harada, T. Ishigaki, H. Kawai and J. Kuwano, *J. Solid State Ionics*, 1998, **108**, 407.
56 L. Sebastian, A. K. Shukla and J. Gopalakrishnan, *Proc. Indian Acad. Sci., Chem. Sci.*, 2001, **113**, 427.
57 (*a*) J. B. Goodenough, H. Y.-P. Hong and J. A. Kafalas, *Mater. Res. Bull.*, 1976, **11**, 203; (*b*) J. B. Goodenough, *Proc. R. Soc. London, Ser. A*, 1984, **393**, 215.
58 H. Y.-P. Hong, *Mater. Res. Bull.*, 1976, **11**, 173.
59 K. K. Rangan and J. Gopalakrishnan, *Inorg. Chem.*, 1995, **34**, 1969.
60 V. Thangadurai, A. K. Shukla and J. Gopalakrishnan, *J. Mater. Chem.*, 1999, **9**, 739.
61 J. Gopalakrishnan and K. K. Rangan, *Chem. Mater.*, 1992, **4**, 745.
62 K. S. Nunjundaswamy, A. K. Padhi, J. B. Goodenough, S. Okada, H. Ohtsuka, H. Arai and J. Yaamaki, *Solid State Ionics*, 1996, **92**, 1.
63 B. L. Cushing and J. B. Goodenough, *J. Solid State Chem.*, 2001, **162**, 176.
64 J. Gaubicher, C. Wurm, G. Goward, C. Masquelier and L. Nazar, *Chem. Mater.*, 2000, **12**, 3240.
65 W. H. Zachariasen, *Z. Kristallogr.*, 1930, **73**, 7.
66 L. Sebastian, J. Gopalakrishnan and Y. Piffard, *J. Mater. Chem.*, 2002, **12**, 374.
67 M. A. G. Aranda, S. Bruque, J. R. Ramos-Barrado and J. P. Attfield, *Solid State Ionics*, 1993, **63–65**, 407.
68 M. A. G. Aranda, J. P. Attfield and S. Bruque, *Angew. Chem., Int. Ed. Engl.*, 1992, **31**, 1090.